Preliminary Report on

450 CPS ELECTRO-HYDROACOUSTIC TRANSDUCER TESTS IN SENECA LAKE

GENERAL DYNAMICS | ELECTRONICS-ROCHESTER

(9) Preliminary Report on

(6) 450 CPS ELECTRO-HYDROACOUSTIC TRANSDUCER TESTS IN SENECA LAKE.

CONTRACT NO (15) N140(70024)70855B new

(11) 15 Jun 62 (12) 35 p.

submitted to:

U.S. NAVY UNDERWATER SOUND LABORATORY

NEW LONDON, CONNECTICUT

attention: HAROLD NASH

Approved by:

J. V. Bouyoucos

Dr. John Bouyoucos
Manager, Hydroacoustics laboratory

D. Y. Keim

D. Y. Keim
Director of Engineering

GENERAL DYNAMICS / ELECTRONICS - ROCHESTER, N.Y.

147 700

ABSTRACT

Low level measurements on the 450 cps Electro-hydroacoustic Research Source are nearly complete, and high level tests have been initiated. Measurements compiled indicate remarkably good agreement with the theoretical directivity pattern and radiation impedance as provided by C. Sherman of the U. S. Navy Underwater Sound Laboratory.

The transducer piston resonant frequency in water is 1 percent lower than the design value. The in-air Q of the piston assembly is approximately 43, and the in-water Q approximately 3.2. On the basis of these Q measurements, the mechano-acoustic efficiency of the piston circuit should be in excess of 90 percent.

From direct measurements of power radiated to the far field and power input to the piston circuit the actual mechano-acoustic efficiency appears to be closer to 55 to 60 percent. An anomalous loss is therefore in evidence when the transducer is submerged in water.

The source of this loss is under investigation. Attention is currently being directed to the piston seal assembly and to the acoustic loss in the seal ring gap when flooded with water. Corrective measures already accomplished should enable the anomalous loss to be alleviated in the event its source is in the seal assembly.

Transducer frequency response measurements at constant voltage input for various tank circuit adjustments have been compared with analog measurements on the transducer equivalent circuit. Good agreement in all cases is in evidence.

The hydroacoustic amplifier currently installed in the transducer has tended to exhibit a bias drift from Class B to Class C operation at the higher drive levels. Whereas efficiency may thereby be increased, the amplifier power capacity is reduced.

Current evidence indicates that with this amplifier the transducer output

power may be limited to 3 to 4 db below the design value of 10 KW. In addition, this amplifier exhibits a slight break point in its linearity response at low power levels.

A modified amplifier of the same class built by General Dynamics/Electronics and tested in the Laboratory under dummy load has developed over 15 KW of acoustic power output, and exhibits no appreciable bias drift or break point.

The test program has been interrupted temporarily to enable modifications to the structure, pneumatic supply, and piston seal assembly to be accomplished. The final portion of the test program is to commence on 13 June and to run through the first week of July.

INTRODUCTION

This report constitutes a preliminary evaluation of test data obtained through 18 May 1962 on the 450 cps Electro-Hydroacoustic Research Source being developed for the U. S. Navy Underwater Sound Laboratory by General Dynamics/ Electronics under Contract N140 (70024) 70855B. Tests on the subject transducer are being conducted at the Seneca Lake Facility of General Dynamics/ Electronics. As of the writing of this report the majority of the low power tests have been completed, and high power tests have been initiated.

The test program was interrupted on 18 May to enable modifications to the supporting structure to be accomplished, per Contract N140 (70024) 73507B, to allow adaption of the transducer mounting framework to the requirements of the USS MALLOY. Advantage has been taken of the structure modification period to correct an air leak in the pneumatic pressure equalization system, to recheck instrument calibration, and to alleviate a potential source of acoustic energy loss in the transducer piston seals. The final test period is to commence on 13 June and run through the first week of July.

SYSTEM DESCRIPTION

The Electro-Hydroacoustic Transducer System is illustrated in Figure 1. The transducer incorporates two four-foot diameter hemispherical, massive pistons mounted back to back on extensional spring elements. The pistons are driven in phase opposition by acoustic forces which must range upwards of 50,000 pounds peak in order to deliver 10 KW of acoustic energy to a radiation load. The driving force is developed by a two-stage hydroacoustic amplifier, mounted within the transducer as shown in Figure 2, whose function is to convert the energy contained in the flow of a hydraulic fluid under pressure to acoustic energy. This conversion process is accomplished by a method of flow switching or modulation analogous to electronic DC to AC power conversion practice. The power stage of the hydroacoustic amplifier for this particular transducer operates as a Class B single ended amplifier. The acoustic signal generated at the amplifier output is essentially a replica of a low-level electrical excitation signal input which activates the amplifier's first stage.

The transducer illustrated in Figure 1 is mounted along with a hydraulic power supply and a pneumatic pressure equalization supply in a structure which may be suspended from a single cable from a surface vessel, or be bottom mounted. The hydraulic supply includes a variable volume delivery pump and motor assembly mounted within a cylindrical oil-filled reservoir.

The suspension cable is employed to transmit 3 Ø, 440 volt, 60 cps power to the hydraulic supply and a low level (below 20 watts) excitation signal to the hydroacoustic amplifier. Additional leads in the cable provide for various control and monitoring functions which are displayed at the control console.

The basic design characteristics of the source, as required under the specification, include an acoustic power output of 10 KW, a center frequency in the vicinity of 450 cps, a bandwidth of 25 percent, an essentially omnidirectional directivity pattern, an overall efficiency from electrical mains to acoustic output of better than 10 percent, and an operating depth capability to 1000 feet.

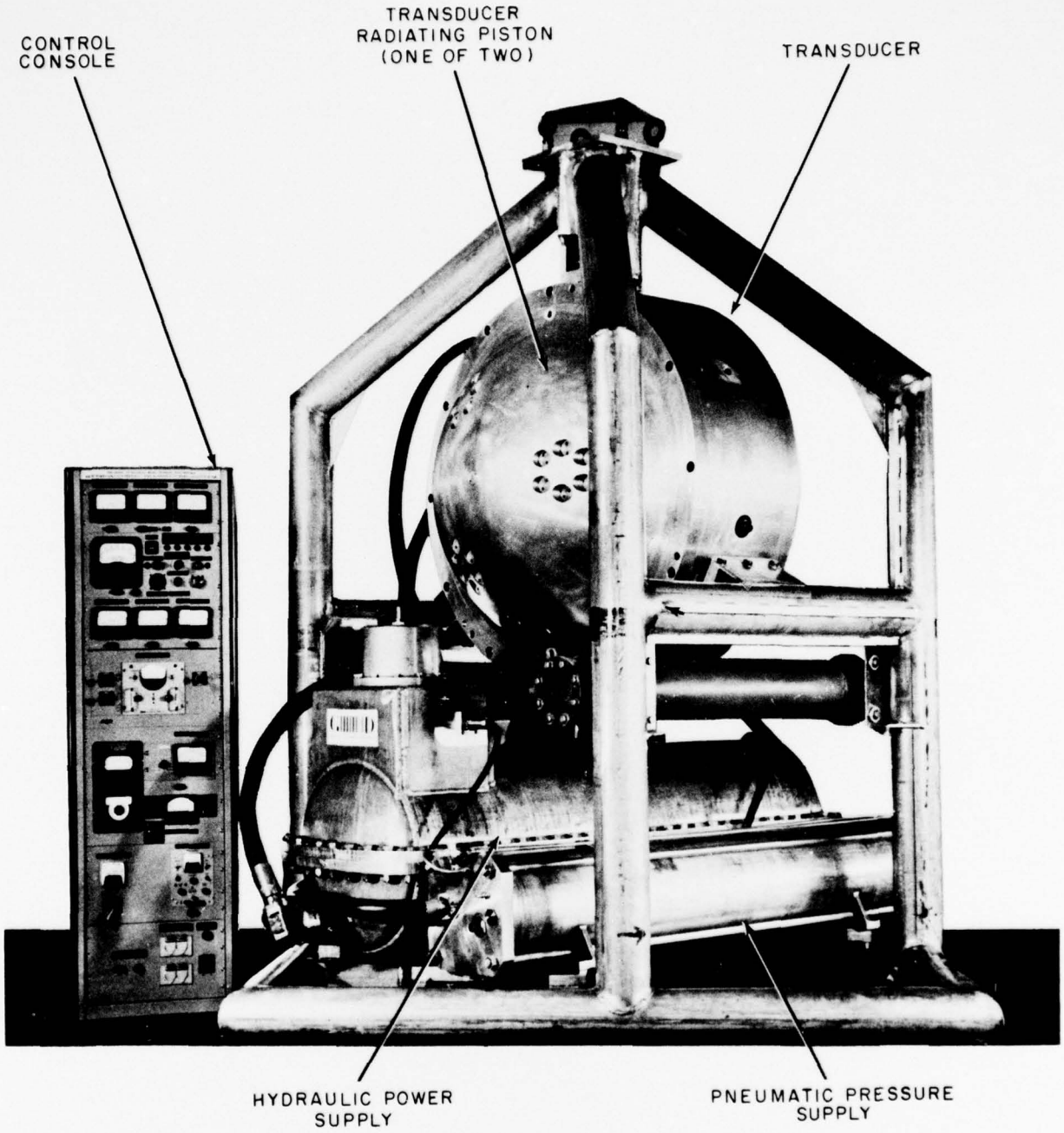

Electro-hydroacoustic transducer system.

Figure 1.

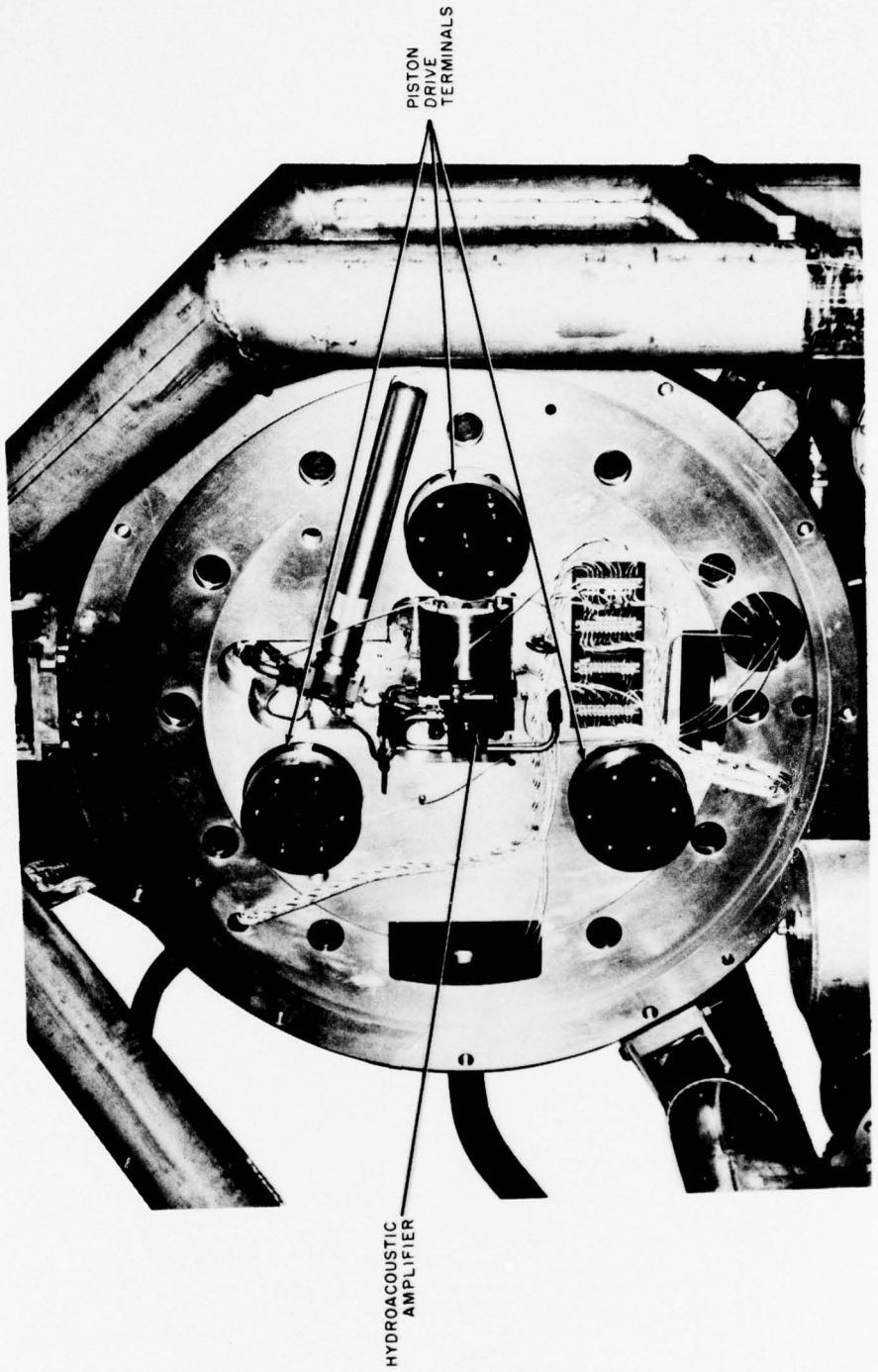

View of the transducer with radiating piston removed.

Figure 2.

Figures 3 and 4 illustrate the transducer being readied for tests at the Lake Seneca Test Facility. The test barge is anchored in 500 feet of water. Due to the length of test cable available, the transducer for these tests cannot be submerged to depths greater than approximately 160 feet or 15 wavelengths.

The load capacity of the handling gear on the barge exceeds 35 tons. The transducer weighs in the vicinity of 6 tons.

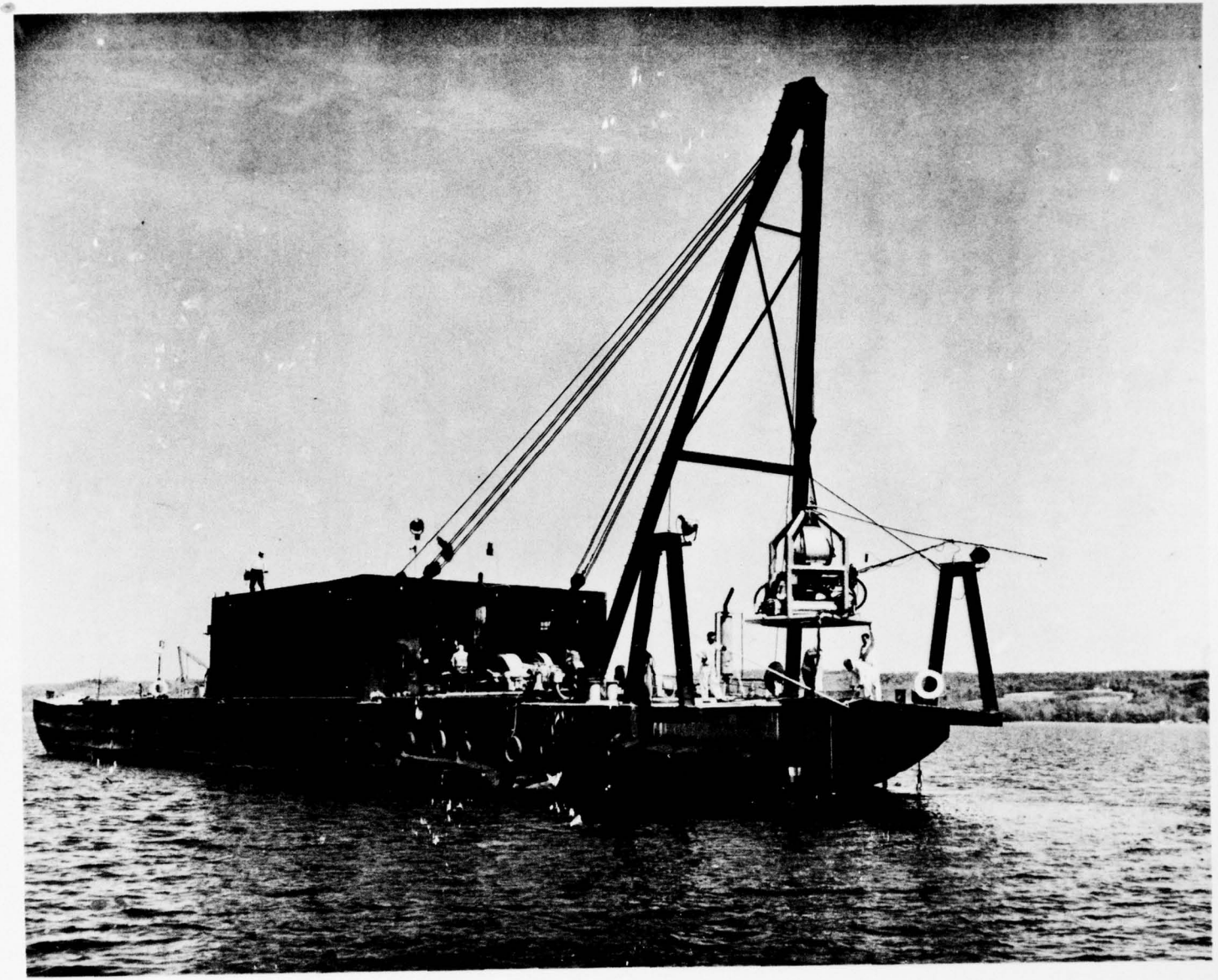

Figure 3. Transducer being readied for testing at the Seneca Lake Test Facility.

Figure 4. Transducer being fitted with temporary boom for hydrophone mounting.

TEST RESULTS

As noted in the Introduction, this report of test results covers only a portion of the projected test program. Highlights of the data obtained to date will be presented to enable the progress under the test program to be set forth. A more complete discussion of results and of test methods will be included in the final report.

Data to be presented here will include piston response in air and in water at constant drive force, uniformity of piston motion, directivity, transducer response at constant voltage input, correspondence between transducer measurements and circuit analog measurements, transducer linearity, and mechano-acoustic efficiency. The report will conclude with a discussion of the expected power output capability of the existing amplifier, and of means for improving overall performance.

The transducer has been instrumented to enable measurement of the distribution of velocity over the pistons, and of the internal acoustic pressure levels at the output terminals of the hydroacoustic amplifier and at the drive terminals of the pistons.

By adjusting the input excitation signal level to maintain constant acoustic signal level at the drive terminals as a function of frequency, the series tuned response of the piston circuit can be obtained at constant drive force.

Figure 5 illustrates the measured velocity vs frequency response of the pistons at constant drive force with the transducer in air. A pneumatic pressure differential of approximately 10 psi is maintained across both pistons and piston seals to simulate typical pneumatic pressure equalization conditions. The resonant frequency occurs at approximately 514 cps as against a design in-air resonance of approximately 518 cps. The bandwidth is roughly 12 cps giving an in-air Q of about 43. The resonant frequency and Q are found to be essentially independent of signal level over the range of design velocities.

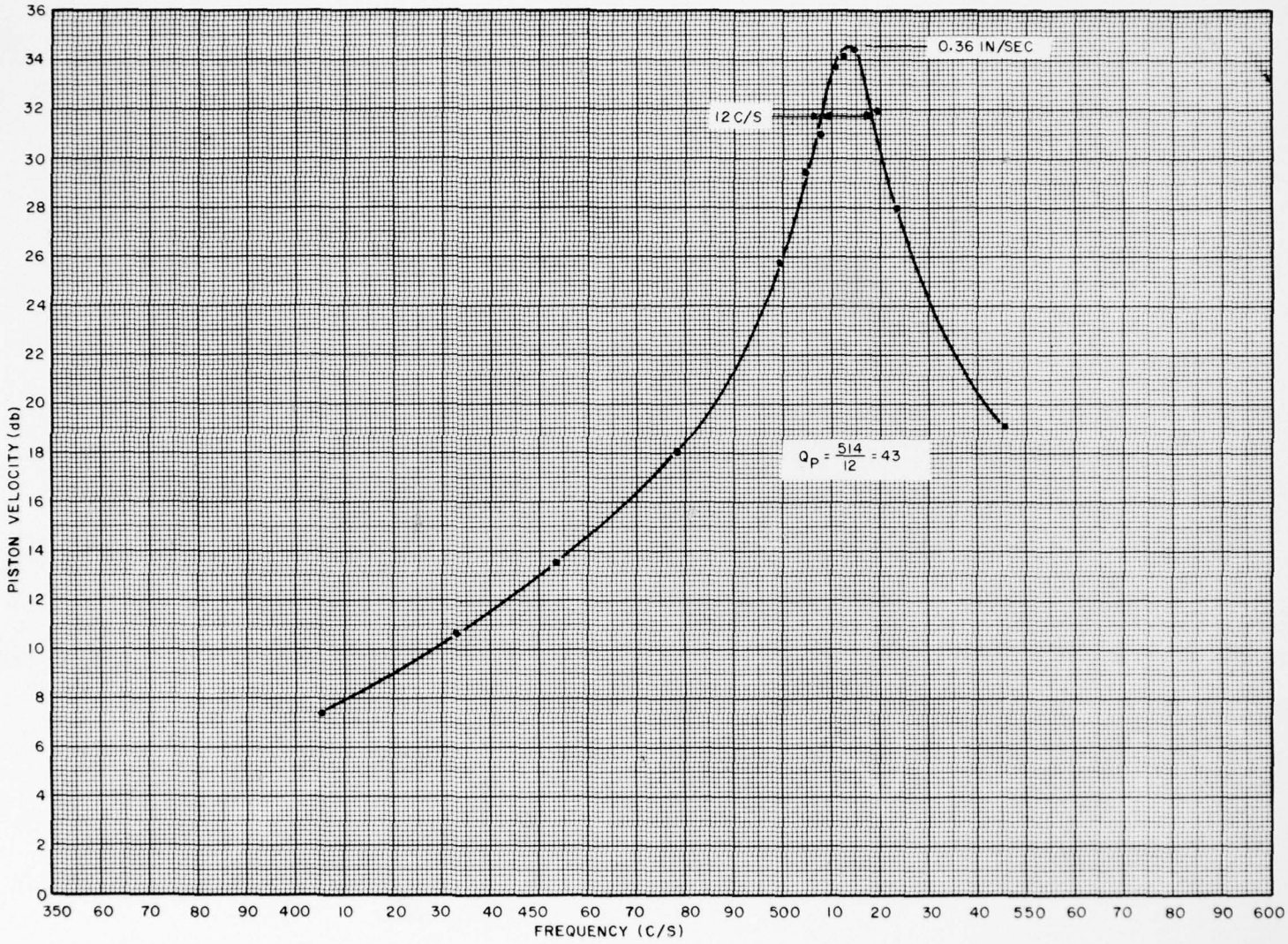

Figure 5.

Transducer piston velocity vs. frequency at constant drive force with transducer in air. The pneumatic pressure differential across the pistons and the pistons seals is maintained at approximately 10 psi to simulate operating conditions. Velocity scale arbitrary.

With the transducer submerged to a depth of 15 wavelengths (approximately 160 feet), the piston velocity vs frequency response at constant drive force is that shown in Figure 6. The resonant frequency as defined by the condition of zero phase between the drive force and piston velocity occurs approximately at 445 cps as against a design resonance of 450 cps. The bandwidth is approximately 140 cps yielding an equivalent Q of about 3.2. This is low compared to the expected value of nearly 5. This discrepancy is to be discussed subsequently.

Figure 7 illustrates the relative motion of various points on the transducer pistons and the center reference biscuit, all referred to the velocity, V_2, at an instrumented drive terminal, with the transducer submerged to 15 wavelengths. The motion of the centers of the two opposing pistons, V_1 and V_5, can be seen to exceed the drive terminal velocity, V_2, by about three quarters of a db on the average. It is to be noted that the velocities of the centers of the opposing pistons are matched to within a few tenths of a db over the entire frequency range of interest.

Whereas the velocity of the pistons centers exceed the drive terminal velocity, the edge velocity V_3 is a few tenths of a db less than the drive terminal velocity.

The motion of the center biscuit against which the two pistons move in phase opposition is given by V_4. The appropriate scale for V_4 is on the right of Figure 7. Over the major portion of the frequency range of interest it can be seen that the center biscuit motion is of the order of 20 db below the drive terminal velocity. This constitutes further evidence of the matching of the masses and resonant frequencies of the two piston assembly.

On the whole, the measurements indicate that the pistons are exhibiting primarily rigid body motion in accordance with design.

Figure 8 exhibits the directivity pattern of the transducer in the horizontal plane. The solid curve is the theoretical directivity pattern for two hemispherical

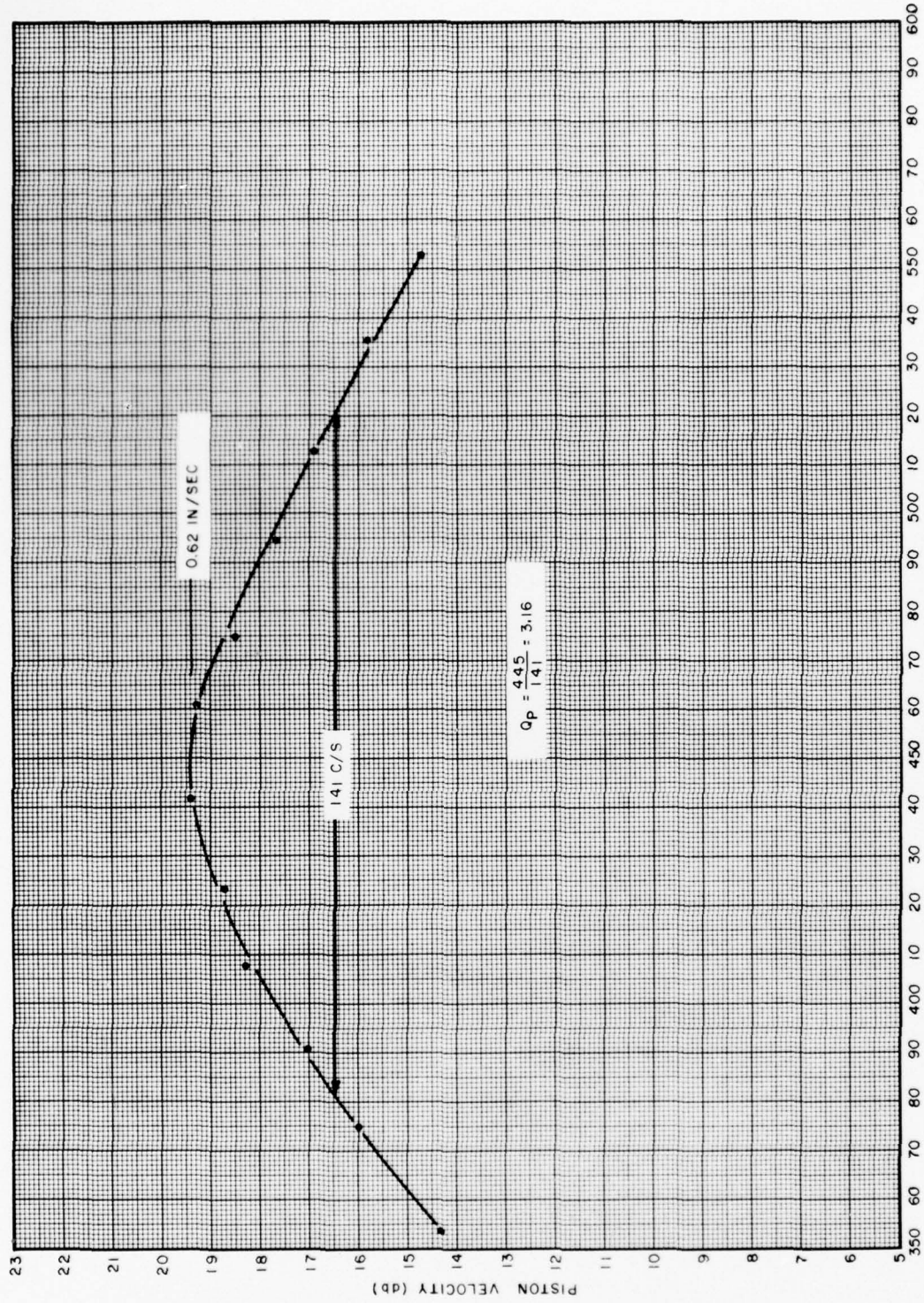

Transducer piston velocity vs. frequency at constant drive force with transducer submerged to 15 wavelengths below water surface. Velocity scale arbitrary.

Figure 6.

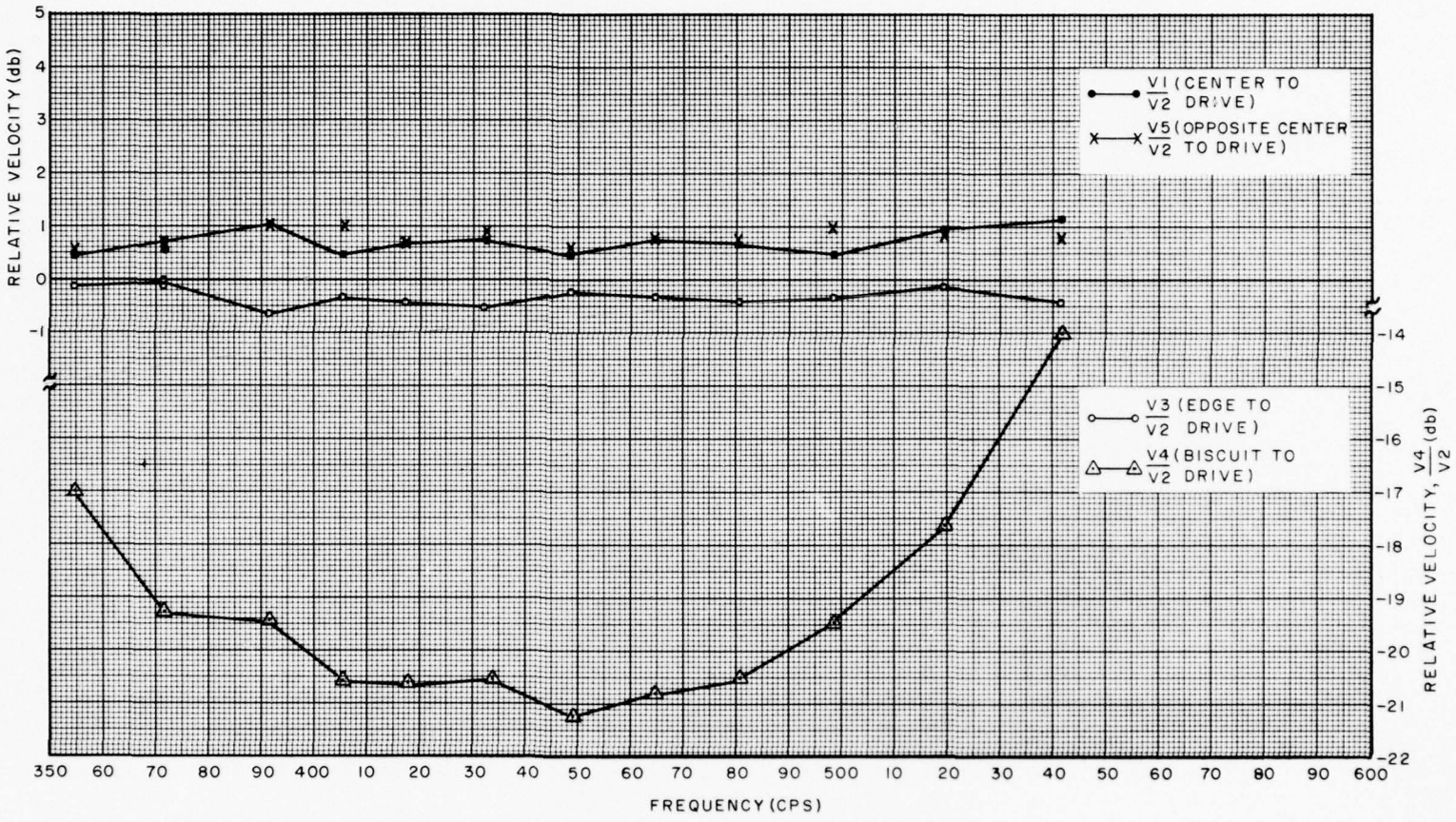

Figure 7.

Relative motion of various points on the transducer pistons and central biscuit referred to an instrumented drive terminal vs. frequency. Transducer submerged to 15 wavelengths.

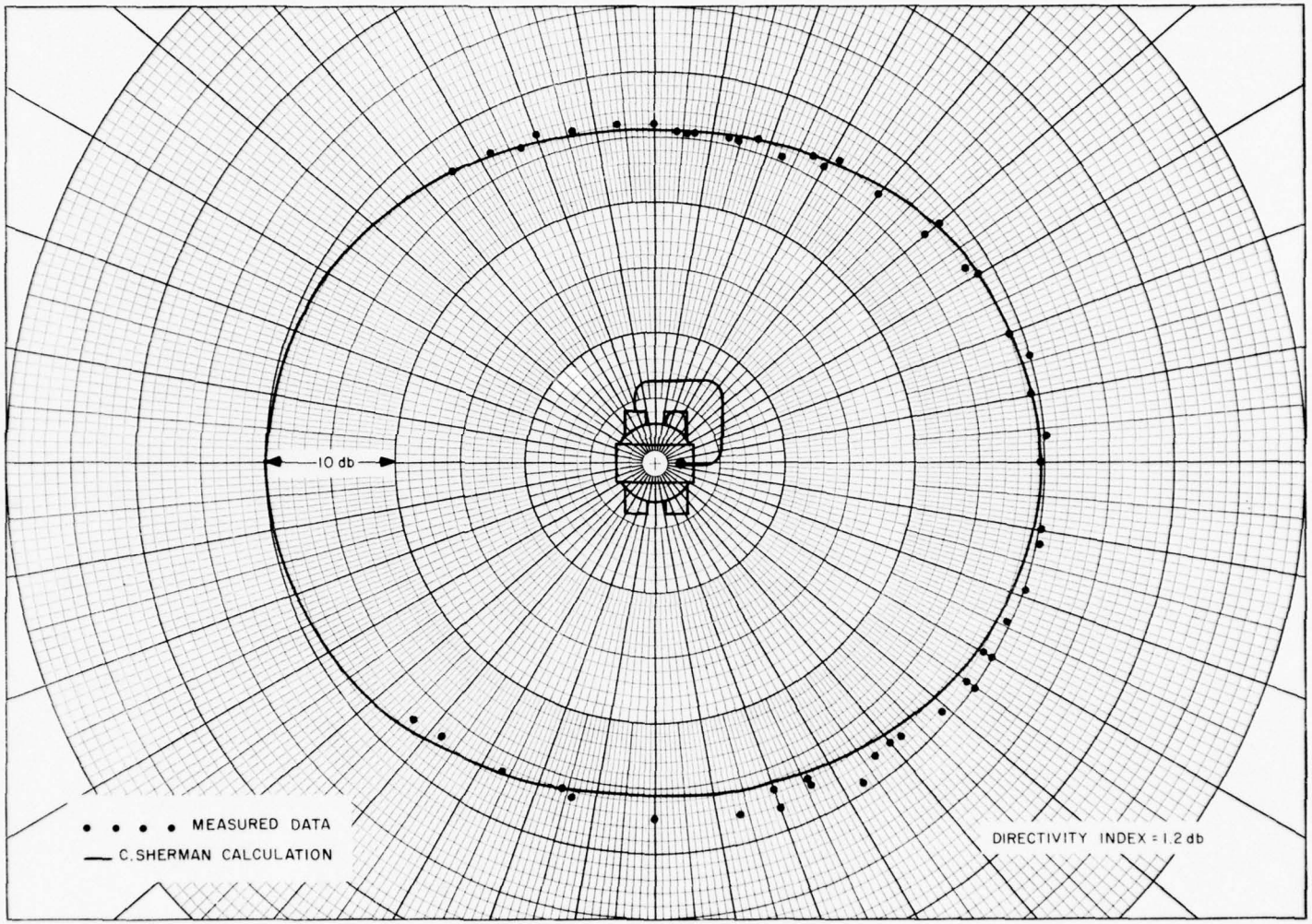

Figure 8. Directional response of the transducer in the horizontal plane compared with the theoretical directivity. Transducer was submerged to a depth of 10 wavelengths, and pulse measurement techniques were employed.

pistons driven back to back for ka = 1.2, as provided by C. Sherman of the Underwater Sound Laboratory. The points constitute measurements made at 15 yards from the transducer center with a hydrophone mounted on a rotating boom whose angular position was read out with a potentiometer. The missing portion of datum points is due to the 270 degree rotation limit of the particular potentiometer employed. Additional datum points should be obtained in the final phases of the test program.

For the directivity measurements the transudcer was suspended at 10 wavelengths below the surface and pulse measurements were employed to avoid interference from surface reflections.

The calculated directivity index is 1.2 db, and the location of maximum pressure is at 90 degrees to the piston axis. The reduction in on-axis pressure arises from the fact that the extreme surfaces of the two hemispheres are spaced approximately 1/3 of a wavelength apart, resulting in a degree of on-axis cancellation. The theoretical minimum to maximum pressure amounts to 4-1/2 db.

The agreement between the theoretical curve and experimental points is further evidence of the piston-like motion of the hemispheres, and indicates that the structure and power supplies in the vicinity of the transducer are not introducing significant reflections.

The curves presented in Figure 9 constitute one of the first sets of measurements on far field pressure, piston velocity and drive terminal pressure vs frequency for constant voltage input to the transducer. Since the transducer circuit is closely related to a constant-k half section bandpass filter, the drive terminal pressure response should exhibit two humps on either side of center frequency. The asymmetry in the drive terminal pressure is indicative of a slight degree of stagger tuning of the parallel resonant amplifier tank circuit with respect to the series resonant transducer piston circuit.

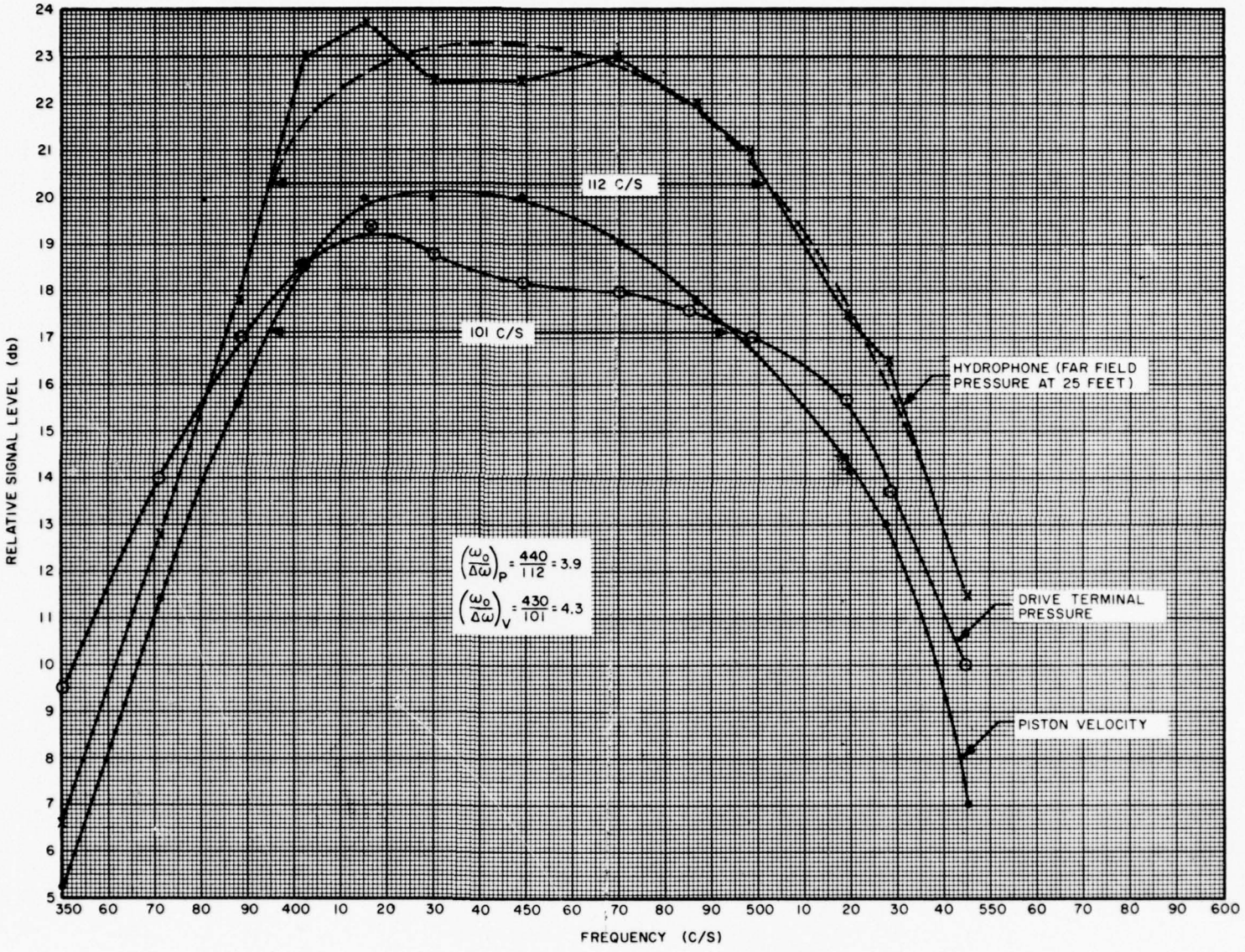

Figure 9.

Relative response of piston velocity, drive terminal pressure, and far field pressure vs. frequency for constant voltage input to the transducer. Transducer submerged 15 wavelengths. CW measurements.

It is to be observed that the hydrophone pressure signal exhibits a fluctuation with frequency not present in the piston velocity or drive terminal pressure signals. The hydrophone output fluctuation was observable in many of the early measurements in which the hydrophone was suspended on its own cable separately from the transducer and during which steady state or CW measurements were conducted. The reasons for the fluctuations are not yet fully understood, but it is hypothesized that the variability may arise from a combination of hydrophone drift with respect to the transducer and cancelling or additive interference from surface reflections as a function of frequency. It may be noted that hydrophone signal fluctuation was markedly reduced upon employing boom mounting for the hydrophone and pulsed measurements, as evidenced by the directivity curve of Figure 8. In the event surface reflection can be shown to be the primary cause of the hydrophone response fluctuations, a plausible explanation for the lack of fluctuation in the piston velocity response stems from the fact that the piston dimensions, in contrast to the hydrophone dimensions, extend over a substantial fraction of a wavelength, thereby enabling a degree of averaging to be achieved.

The piston velocity bandwidth response at constant input voltage is slightly less than would be expected if the design loading on the piston were in fact achieved. It will be recalled that the piston circuit loading is actually greater than anticipated (i.e., the observed bandwidth for constant drive force, Figure 6, is broader than the design bandwidth). The load impedance thereby reflected to the transducer tank circuit turns out to be higher than the design value, with the net effect that the tank circuit load is under the design level. The tank circuit response then controls the overall bandwidth.

Although the piston velocity bandwidth is somewhat under 25 percent, the power response, as indicated by the far field pressure measurements, has a bandwidth slightly in excess of 25 percent. The difference is attributable to the increase in radiation resistance with frequency over the bandwidth, as a result of the piston ka being placed in the vicinity of unity.

In the event the anomalous loading on the piston circuit is alleviated through work currently in progress, the system bandwidth at constant voltage input will increase.

In view of the anomalous loading, it was felt desirable to ascertain whether the analog circuit that has been established for the transducer would in fact track the measured results. The analog circuit was modified to accommodate the measured piston circuit impedance as seen at the drive terminals, and then response curves of piston velocity and drive terminal pressure for constant excitation voltage were obtained for various adjustments of the tank circuit. These same tank circuit adjustments were made on the transducer and its performance measured. The comparison of transducer measurements with analog results is presented in Figures 10 through 13. The test data presented in Figure 10 are for the same conditions as in Figure 9. The data in Figures 11, 12, and 13 relate to a modified tank circuit in which the equivalent L and C are varied by prescribed amounts.

The general agreement between the analog results, represented by the smooth curves, and the datum points, representing transducer measurements, indicates that the analog circuit is a reasonably good representation of the actual transducer circuit. The final transducer circuit settings will be close to those defined by the results of Figure 9 and 10.

Figure 14 illustrates the variation of hydrophone signal pressure, drive terminal pressure, and piston velocity at the piston circuit resonant frequency, as a function of excitation current. The break point in the curves is a characteristic of the first stage of the particular hydroacoustic amplifier currently in the transducer. The acoustic power output to the far field represented by the maximum datum points on the graph is about 2 KW. A linear extrapolation of the curves to the 10 KW level would require a further increase of excitation signal of 7 db, or to a relative excitation level of 40 db on the graph.

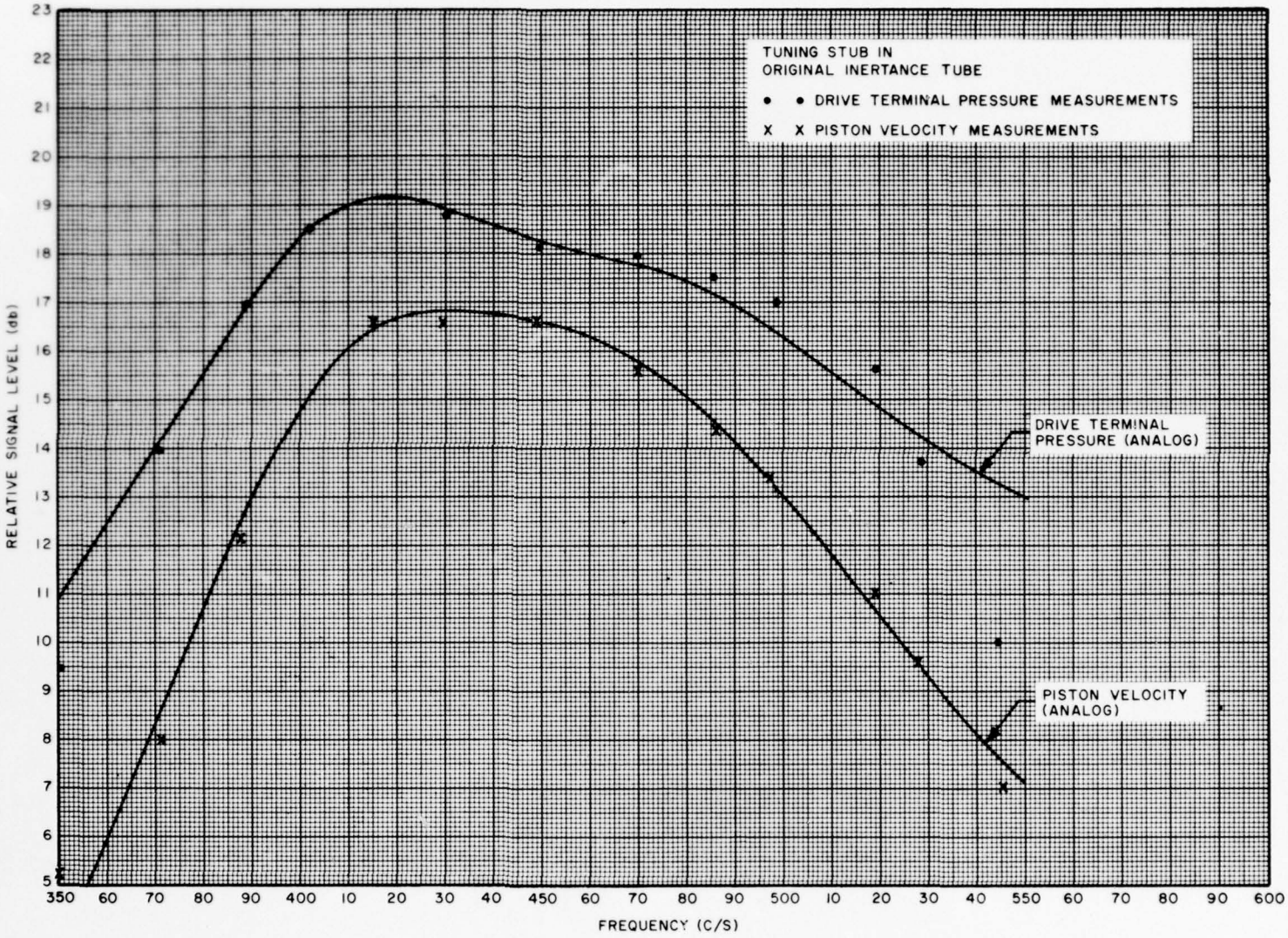

Figure 10.

Comparison of measurements of piston velocity and drive terminal pressure vs. frequency for constant voltage input with analog measurements on the equivalent transducer circuit.

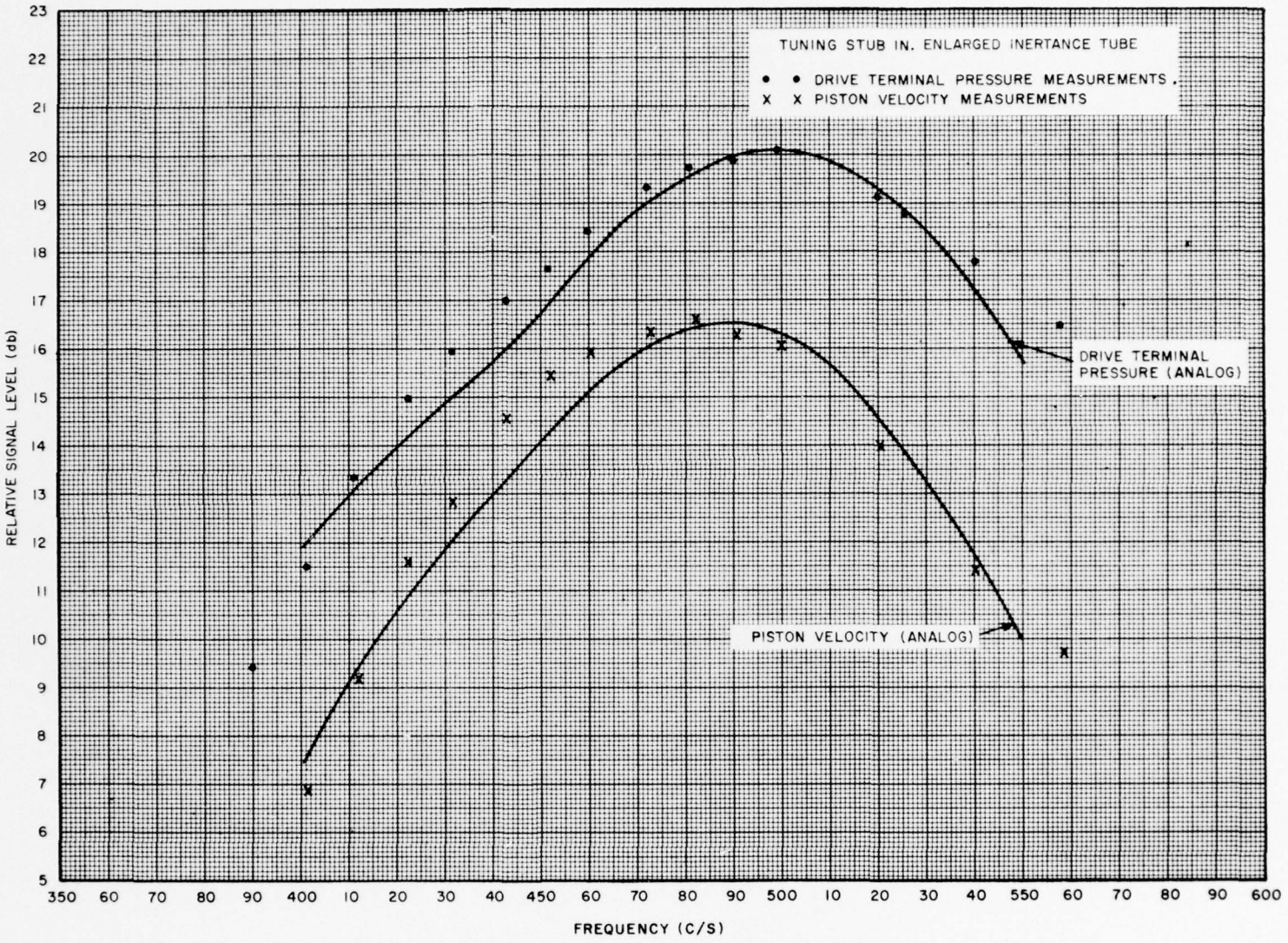

Figure 11.

Comparison of measurements of piston velocity and drive terminal pressure vs. frequency for constant voltage input with analog measurements on the equivalent transducer circuit. Transducer tank circuit L and C are modified.

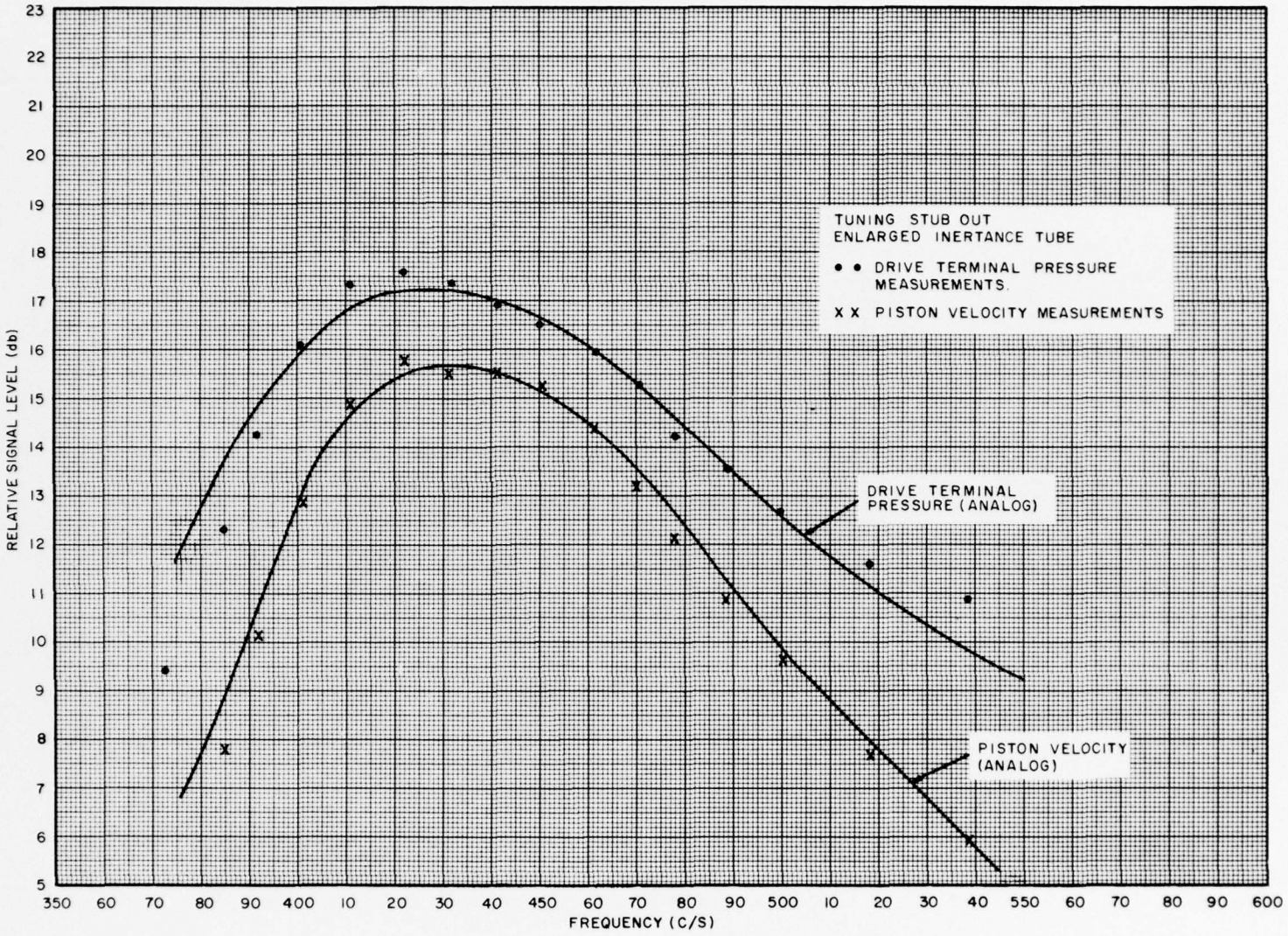

Figure 12.

Comparison of measurements of piston velocity and drive terminal pressure vs. frequency for constant voltage input with analog measurements on the equivalent transducer circuit. Transducer tank circuit L and C are modified.

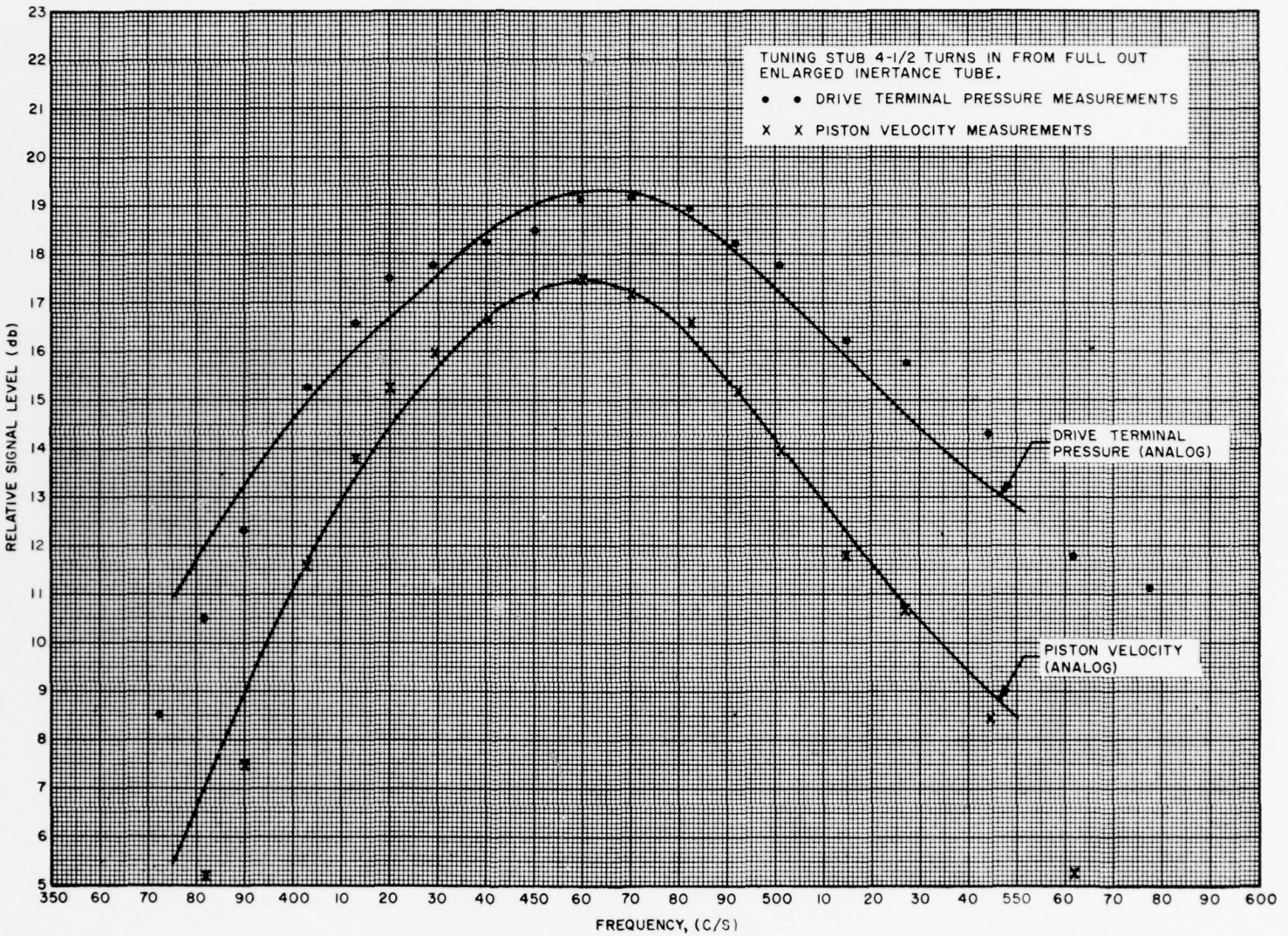

Figure 13.

Comparison of measurements of piston velocity and drive terminal pressure vs. frequency for constant voltage input with analog measurements on the equivalent transducer circuit. Transducer tank circuit L and C are modified.

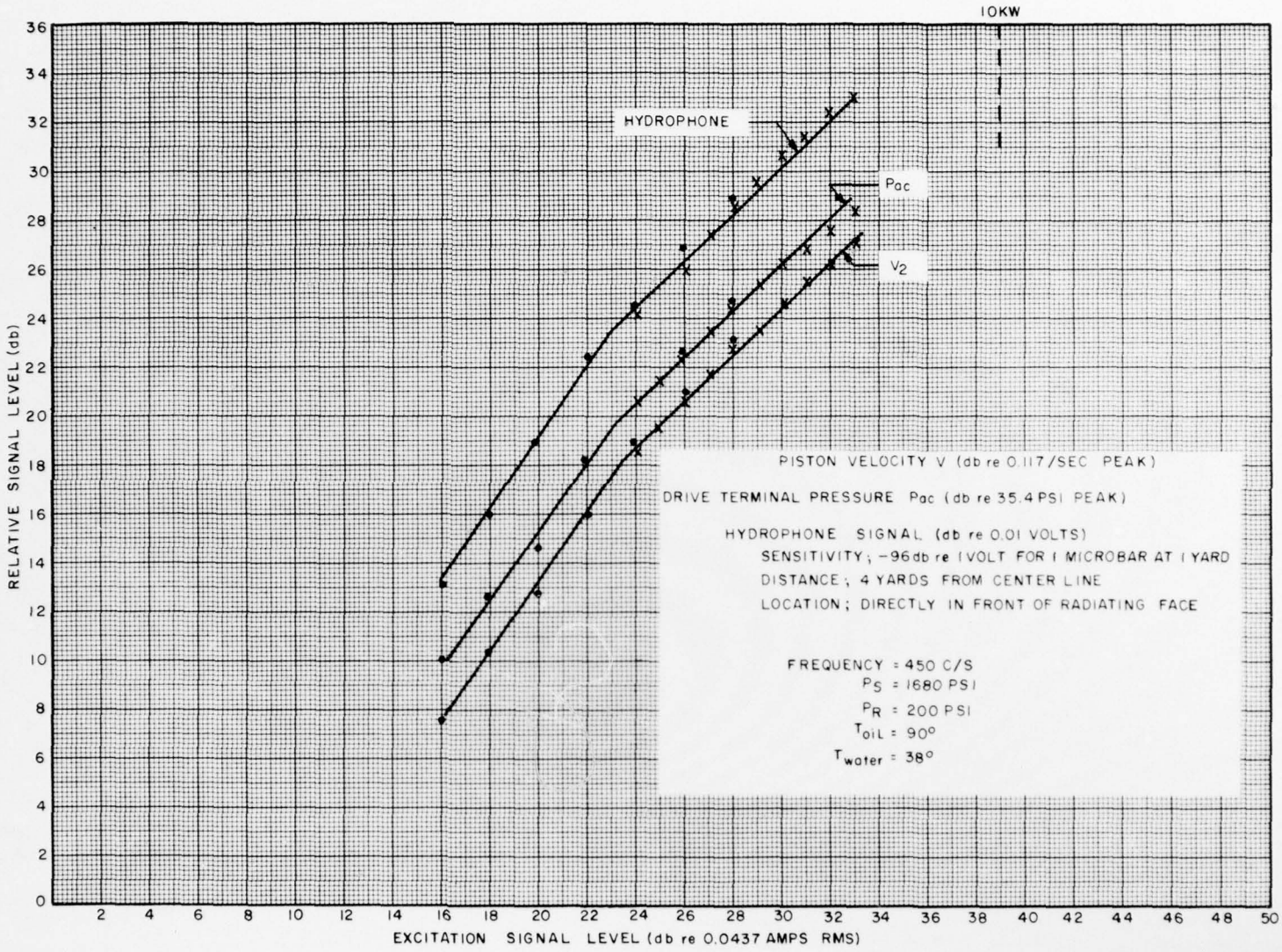

Figure 14.

Piston velocity, drive terminal pressure, and hydrophone output vs. excitation current input to transducer at 450 cps. Transducer submerged to 10 wavelengths.

Current evidence indicates that with the anomalous loading behavior and as a result of the particular characteristics of the present amplifier, the probable safe output power level from the transducer will be on the order of 3 db down from the 10 KW design value. The present amplifier has exhibited in the Laboratory a tendency for the power stage bias to drift from Class B operation toward Class C at the higher excitation levels. Whereas, this drift will tend to increase efficiency, it also reduces power handling capacity.

A modified amplifier of essentially the same design built by the Laboratory under Company sponsorship has not exhibited this bias shift and has developed over 15 KW of acoustic power output into our Laboratory dummy load. In addition, this amplifier does not exhibit the break point illustrated in Figure 14.

The transducers tests to date have not exceeded the 2 KW level, since it has been felt desirable first to check the calibration of some of the internal instrumentation. This calibration check has been accomplished during the aforementioned structure modification period, and further investigation of high power performance is about to commence.

COMPUTATION OF MECHANO-ACOUSTIC EFFICIENCY, EFFECTIVE RADIATION RESISTANCE, AND DISCUSSION OF ANAMALOUS LOSS

Several methods will be employed to estimate the mechano-acoustic efficiency of the transducer piston circuit. These methods include a direct comparison of the power radiated to the far field with the power delivered to the drive terminals, and, alternatively, a comparison of in-air and in-water Q's. In addition, the radiation resistance derived from far field measurements will be compared with theory.

During the course of the directivity measurements in which a pulse technique was employed to avoid interference from surface reflections, the following conditions were established at resonance:

Reference piston velocity, V_2, at drive terminal	4.32 cm/sec (peak)
Drive terminal acoustic pressure, P_{AC}	48.0×10^6 dynes/cm^2 (peak)
Atlantic Research LC 32 hydrophone output at maximum of directivity pattern, and at 15 yards	-31.92 db re 1 volt
Spreading loss (15 yards)	23.52 db
Hydrophone output corrected to 1 yard	-8.40 db re 1 volt
Hydrophone sensitivity with attached cable	-111 db re 1 volt/dyne/cm^2
Signal pressure corrected to 1 yard	102.6 db re 1 dyne/cm^2
Directivity index	1.2 db
Source level	101.4 db
Radiated acoustic power (for reference piston velocity of 4.32 cm/sec)	955 watts

From the above-measured power in the far field, we may extrapolate back to establish the average specific acoustic impedance, r_S, presented to the

pistons, since the radiated power W_{AC} is given by

$$W_{AC} = 1/2 \hat{V}_2^2 r_S A_{PT} \quad (1)$$

where A_{PT} is the total piston area (2.34×10^4 cm^2).

From Equation 1, r_S may be solved to obtain

$$r_S = \frac{2 W_{AC}}{\hat{V}_2^2 A_{PT}} \quad (2)$$

or

$$r_S = \frac{2 \times 955 \times 10^7}{(4.32)^2 \times 2.34 \times 10^4} = 0.349 \times 10^5 \text{ dynes sec/cm}^3 \quad (3)$$

and $r_{S/\rho c} = 0.292$

C. Sherman has calculated the radiation impedance presented to two hemispherical pistons mounted back to back and driven in phase opposition, and for the case at hand, his results are,* for the design ka = 1.16,

$$\mathcal{Z}_{S/\rho c} = 0.29 + j\ 0.32 \quad (4)$$

It is evident that the resistive terms are in excellent agreement. Furthermore, in view of the close agreement between the design and observed in-water resonant frequencies, the reactive term of equation (4) must be an accurate expression of the observed value.

The power to the piston circuit at piston resonance is given by the expression

$$W_{AC} = 1/2 \hat{P}_{AC}, \times \hat{V}_2 \times A_{DT} \quad (5)$$

*Letter communication dated 3 January, 1961, Serial 912.1-2 from C. Sherman to J.V. Bouyoucos

where P_{AC} is the peak drive terminal acoustic pressure, V_2 is the peak drive terminal piston velocity, and A_{DT} is the total drive terminal area.

As $A_{DT} = 167.5\ cm^2$, and from the above reference data,

$$W_{AC} = 1/2 \times 4.8 \times 10^7 \times 4.32 \times 1.675 \times 10^2$$

$$= 1.73\ KW \tag{6}$$

In addition, one can show that the effective average specific acoustic radiation resistance presented to the pistons at resonance is given by

$$r_{S_{eff}} = \frac{P_{AC}}{V_2} \times \frac{A_{DT}}{A_{PT}} \tag{7}$$

where A_{PT} is the total piston area. As the ratio A_{DT}/A_{PT} for this transducer is 0.724×10^{-2}, $r_{S_{eff}}$ becomes

$$r_{S_{eff}} = \frac{4.8 \times 10^7}{4.32} \times 0.724 \times 10^{-2} = 0.805 \times 10^5 \text{ dynes sec/cm}^3$$

$$\text{or} \quad r_{S_{eff}/\rho c} = 0.56 \tag{8}$$

As a check on the above calculations we may employ the approximate expression

$$r_{S_{eff}} = \frac{\omega_o (M_{PT} + M_{WT})}{Q A_{PT}} \tag{9}$$

where ω_o is the circular resonant frequency and $(M_{PT} + M_{WT})$ is the sum of the piston and water mass. Equation (9) would normally be an exact expression defining Q unambiguously if r_S and M_{WT} were to remain constant with frequency over the transducer bandwidth. In view of the close agreement between the observed and the design resonance frequency it can be assumed that the design accession to inertia is valid whence it can be shown that $(M_{PT} + M_{WT}) = 2.0 \times 10^6$ grams.

Hence

$$r_{S_{eff}} = \frac{2.82 \times 10^3 \times 2.0 \times 10^6}{3.16 \times 2.34 \times 10^4} = 0.764 \times 10^5 \text{ dynes sec/cm}^3 \qquad (10)$$

or

$$r_{S_{eff}/\rho c} = 0.53$$

Using this latter value for $r_{S_{eff}}$ the power transferred through the piston circuit becomes

$$W_{AC} \quad 1/2 \, \hat{V}_2^2 \quad r_{S_{eff}} \quad A_{PT}$$

$$= 1/2 \, (4.32)^2 \times 0.764 \times 10^5 \times 2.34 \times 10^4$$

$$= 1.65 \text{ KW} \qquad (11)$$

The results for the reference velocity above defined are summarized below.

Far field radiated power	955 watts
Power delivered to piston drive terminals (Eq. 16)	1.73 KW
Estimate of power transferred through piston circuit based on Q (Eq. 11)	1.65 KW
Mechano-acoustic efficiency, η_{ma}	$\frac{.955}{1.73} \times 100 = 55$ percent $\frac{.955}{1.65} \times 100 = 58$ percent
Normalized design specific acoustic impedance, $r_{S/\rho c}$	0.29
Calculated $r_{S/\rho c}$ based upon far field power [Eq. (3)]	0.292
Calculated $r_{S_{eff}/\rho c}$ based upon drive terminal measurement [Eq. (8)]	0.56
Estimated $r_{S_{eff}/\rho c}$ based upon measured bandwidth Eq. [(10)]	0.53

It is evident that a series resistance above and beyond the true radiation resistance is being presented to the piston circuit to absorb over 40 percent of the power delivered to the drive terminals.

Surprisingly, this resistance does not appear in the in-air Q measurement on the transducer! The mechano-acoustic efficiency based upon in-air to in-water Q measurements is given approximately by the expression.

$$\eta_{ma} = \frac{\frac{\omega_a}{\omega_w} \times \frac{1}{Q_w}}{\frac{1}{Q_a} + \frac{\omega_a}{\omega_w} \times \frac{1}{Q_w}} \tag{12}$$

where ω_a is the circular in-air resonant frequency, ω_w is the in-water resonant frequency, Q_a is the in-air Q, and Q_w is the in-water Q. As Q_a = 43, Q_w = 3.2, $\omega_a = 2\pi \times 514$, and $\omega_w = 2\pi \times 445$

$$\eta_{ma} = \frac{\frac{514}{445} \times \frac{1}{3.2}}{\frac{1}{43} + \frac{514}{43} \times \frac{1}{3.2}} \times 100 = 94\% \tag{13}$$

It is to be noted that in design the mechano-acoustic efficiency was estimated to be 80 percent, a figure which falls between that of Eq. (13) and the value obtained from direct power measurements.

As a result of the low measurement of in-air loss, an energy sink has been sought which depends upon the transducer being submerged in water. In view of the uniformity of the directivity pattern a localized sink in the structure, hose fittings, etc., does not appear reasonable.

A potential source of energy loss has been found to exist in the piston seal assembly. When the seal gap is flooded with water, the O ring may act as a piston source to pump water back and forth in the gap at velocities far in excess of the piston velocity. Estimates indicate that the observed power loss could in

large part be attributed to viscous losses in this gap. As these losses are a function of the cube of the inverse gap thickness, a small change in gap thickness can have substantial effect.

During the course of the structure modification, the gap width has been increased. Subsequent measurements will determine whether the anomalous loss can be attributed to this source.

THE REMAINING TEST PROGRAM

The remaining test program will be devoted to clarifying and minimizing, if possible, the anomalous loss problem in the piston circuit, to the obtaining of further high power data, harmonic distortion data, data on performance with band-limited pseudo random noise input, impedance circle data, overall power conversion efficiency, power supply noise and other pertinent information. A final report will include such data, together with a more detailed analysis of the information presented herewith.

CONCLUSIONS

From the measurements completed to date it is evident that the transducer is performing by and large in accordance with design. In the event the anomalous loss behavior can be corrected, it can be stated that the transducer performance will have exceeded expectations in several respects. It must be recalled that this is the first electro-hydroacoustic transducer ever to be constructed, embodying fully the principles set forth in Reference 1.

The main problem area currently envisioned appears to rest primarily in the hydroacoustic amplifier (See Figure 2) that is now mounted in the transducer. This amplifier is a first generation amplifier, and its performance, as previously noted, has already been exceeded by a modified version built by GD/E and currently under test in the Hydroacoustics Laboratory.

It is hoped that the opportunity will arise to enable either the amplifier currently in the transducer to be updated if feasible, or to provide an amplifier which will permit the transducer to develop its full power capability consistent with the design specification.

REFERENCES

1. "Hydroacoustic Transduction - A Survey", J. V. Bouyoucos, Journal of Underwater Acoustics 11, 327 - 360 (July 1961)
2. "Electro-hydroacoustic Transducers for a System of Research Sources", Proposal ED60-4130 submitted to the U. S. Navy Underwater Sound Laboratory on 17 June 1960.